### Title

Noninvasive in vivo monitoring of methemoglobin formation and reduction with broadband diffuse optical spectroscopy




### Journal

Journal of Applied Physiology, 100(2)

### ISSN

8750-7587



### Authors

Lee, Jangwoen
El-Abaddi, Naglaa
Duke, Andrew
et al.



### Publication Date

2006-02-01

### DOI

10.1152/japplphysiol.00424.2004

*J Appl Physiol* 100: 615–622, 2006.
First published October 13, 2005; doi:10.1152/japplphysiol.00424.2004.

# Noninvasive in vivo monitoring of methemoglobin formation and reduction with broadband diffuse optical spectroscopy

**Jangwoen Lee,[1] Naglaa El-Abaddi,[2] Andrew Duke,[2] Albert E. Cerussi,[1] Matthew Brenner,[1,2] and Bruce J. Tromberg[1]**

[1]*Laser Microbeam and Medical Program, Beckman Laser Institute and* [2]*Division of Pulmonary Medicine, Department of Medicine, University of California, Irvine, California*

**Lee, Jangwoen, Naglaa El-Abaddi, Andrew Duke, Albert E. Cerussi, Matthew Brenner, and Bruce J. Tromberg.** Noninvasive in vivo monitoring of methemoglobin formation and reduction with broadband diffuse optical spectroscopy. *J Appl Physiol* 100: 615–622, 2006. First published October 13, 2005; doi:10.1152/japplphysiol.00424.2004.—We present noninvasive, quantitative in vivo measurements of methemoglobin formation and reduction in a rabbit model using broadband diffuse optical spectroscopy (DOS). Broadband DOS combines multifrequency frequency-domain photon migration (FDPM) with time-independent near infrared (NIR) spectroscopy to quantitatively measure bulk tissue absorption and scattering spectra between 600 nm and 1,000 nm. Tissue concentrations (denoted by brackets) of methemoglobin ([MetHb]), deoxyhemoglobin ([Hb-R]), and oxyhemoglobin ([$HbO_2$]) were determined from absorption spectra acquired in "real time" during nitrite infusions in nine pathogen-free New Zealand White rabbits. As little as 30 nM [MetHb] changes were detected for levels of [MetHb] that ranged from 0.80 to 5.72 μM, representing 2.2 to 14.9% of the total hemoglobin content (%MetHb). These values agreed well with on-site ex vivo cooximetry data ($r^2 = 0.902$, $P < 0.0001$, $n = 4$). The reduction of MetHb to functional hemoglobins was also carried out with intravenous injections of methylene blue (MB). As little as 10 nM changes in [MB] were detectable at levels of up to 150 nM in tissue. Our results demonstrate, for the first time, the ability of broadband DOS to noninvasively quantify real-time changes in [MetHb] and four additional chromophore concentrations ([Hb-R], [$HbO_2$], [$H_2O$], and [MB]) despite significant overlapping spectral features. These techniques are expected to be useful in evaluating dynamics of drug delivery and therapeutic efficacy in blood chemistry, human, and preclinical animal models.

methemoglobinemia; quantitative; rate kinetics; therapeutic monitoring

METHEMOGLOBINEMIA IS AN ALTERED hemoglobin condition resulting from the oxidation of the ferrous moiety within the hemoglobin molecule. This conversion leads to abnormal oxygen affinity, reduced oxygen-carrying capacity, and tissue hypoxia. Methemoglobinemia can be induced by multiple pharmacological and chemical exposures, including nitrites. Fatalities from recreational usages of amyl nitrite (AN) as well as nitrite contamination of well water have been described (5, 6, 36, 37). Significantly elevated levels of methemoglobin have been reported in patients with sepsis (26, 28), infants who develop severe metabolic acidosis (blue baby syndrome), and individuals with rare congenital metabolic anomalies such as glucose phosphate dehydrogenase deficiency (9, 41). In addition, there have been case reports of topical anesthesia, including lidocaine and benzocaine, inducing methemoglobinemia (21, 38, 40). Severe untreated methemoglobinemia can lead to delirium and death. Complaints can be vague, and typical diagnostic testing can be misleading. Therapeutic implications can range from observation to admission into the intensive care unit for further management.

As with other potentially life-threatening illnesses, early recognition of methemoglobinemia is crucial, as is monitoring the effects of therapy. Traditional diagnostic modalities for hypoxemic patients include pulse oximetry, arterial blood-gas analysis, and cooximetry. Pulse oximetry is unreliable in the presence of methemoglobinemia because methemoglobin (MetHb) absorbs light equally well at wavelengths (typically 660 and 940 nm) used to determine oxygen saturation (1, 2, 10, 24). Arterial blood-gas analysis can also be misleading in methemoglobinemia because it will show normal $P_{O_2}$, even in the presence of high MetHb concentration and inaccurate oxygen saturation if values were calculated from the pH and arterial $P_{O_2}$. Cooximetry is generally the preferred laboratory technique for diagnosis of methemoglobinemia, but, because it relies on the absorption spectra of a few wavelengths for the calculation of MetHb concentration, false positive readings can result from the presence of other pigments, such as methylene blue (MB) or sulfhemoglobin, which have high absorption at the methemoglobin absorption peak of 630 nm (11, 32). In addition, cooximetry requires intermittent blood drawing and fresh specimens for analysis because methemoglobin levels can rise with storage (25).

Once formed, methemoglobin can be reduced back to hemoglobin either enzymatically or nonenzymatically via a number of pathways. For drug-induced methemoglobinemia, MB is a standard treatment modality because MB serves as an exogenous electron acceptor and works as a cofactor for NADPH (reduced nicotinamide adenine nucleotide phosphate) reductase to reduce hemoglobin back to the original ferrous state. However, large doses of MB can result in hemolysis and, paradoxically, methemoglobinemia in patients with glucose phosphate dehydrogenase deficiency (17, 34, 41).

Most chemical reactions involving the heme group cause detectable changes in hemoglobin's visible absorption spectrum. The oxidation of hemoglobin results in a marked increase of absorption in the red region of the visible spectrum (600–650 nm). As shown in Fig. 1, methemoglobin has a strong absorption peak at 630 nm (42). This change of absorption spectra due to the formation and reduction of methemoglobin presents an optimal diagnostic platform for broadband diffuse

Address for reprint requests and other correspondence: B. J. Tromberg, Laser Microbeam and Medical Program, Beckman Laser Institute, 1002 Health Sciences Rd. East, University of California, Irvine, CA 92612-1475 (e-mail: bjtrombe@uci.edu).

The costs of publication of this article were defrayed in part by the payment of page charges. The article must therefore be hereby marked "*advertisement*" in accordance with 18 U.S.C. Section 1734 solely to indicate this fact.

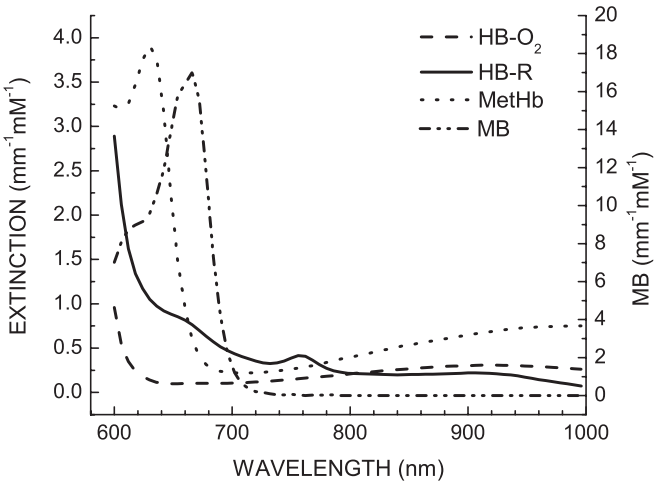


Fig. 1. Extinction coefficient spectra of hemoglobin species in near-infrared wavelengths between 600 and 1,000 nm. Methemoglobin (MetHb) has an absorption peak around 630 nm. $HbO_2$, oxyhemoglobin; Hb-R, deoxyhemoglobin; MB, methylene blue.

optical spectroscopy (DOS) (4, 20, 39). Broadband DOS combines multifrequency frequency-domain (FD) photon migration (FDPM) with time-independent near infrared (NIR) spectroscopy to quantitatively measure bulk tissue absorption and scattering spectra between 600 and 1,000 nm. As a result, broadband DOS can rapidly quantify the in vivo concentrations of multiple tissue chromophores and exogenous dyes such as MB noninvasively (8). Because of the quantitative description of tissue composition, broadband DOS can overcome the shortcomings of existing methemoglobinemia diagnostic modalities while providing additional valuable physiological information.

Previous studies have demonstrated that FDPM can readily detect methemoglobin in tissue phantoms (16) and MB in vivo (8). However, there is little research demonstrating the quantitative evaluation of methemoglobinemia using noninvasive spectrophotometric techniques. Moreover, no quantitative studies have simultaneously monitored the concentration of five chromophores (four endogenous chromophores and MB) in vivo during methemoglobinemia and its response to treatment with MB. The first objective of this feasibility study was to show that a stable in vivo animal model can be created with significant amounts of methemoglobin produced. The second objective was to show that broadband DOS can be used to detect and monitor the formation and resolution of methemoglobinemia. The purpose of this study is to demonstrate that broadband DOS is capable of dynamic monitoring of multiple in vivo tissue chromophores noninvasively with sensitivities necessary for effective therapeutic monitoring.

## MATERIALS AND METHODS

*Broadband diffuse optical spectroscopy.* A broadband DOS instrument was used for the noninvasive in vivo assessment of MetHb formation and reduction. Figure 2 shows a simple schematic diagram of the broadband DOS instrument that combines steady-state (SS) and FD photon migration techniques. The technique for combining multiwavelength FD data with time-independent steady-state (SS) spectroscopy for quantitatively determining absorption ($\mu_a$) and reduced scattering ($\mu_s'$) coefficients over a broad spectral bandwidth has been previously described (4, 20, 39). In brief, broadband DOS employs six laser diodes (661, 681, 783, 823, 850, and 910 nm) and a fiber-coupled avalanche photo diode (APD) detector (Hamamatsu high-speed APD module C5658). The APD detects the intensity-modulated diffuse reflectance signal at modulation frequencies between 50 and 550 MHz after propagating through the tissue. The absorption and reduced scattering coefficients are measured directly at each of the six laser diode wavelengths by using the frequency-dependent phase and amplitude data (4, 20, 30, 39). The reduced scattering coefficient is calculated throughout the NIR by fitting a power law to these six reduced scattering coefficients (18, 27, 35). The power-law fit allows the interpolation of scattering coefficients throughout the NIR. The SS acquisition is a broadband reflectance measurement from 600 to 1,000 nm that follows the FD measurements using a tungsten-halogen light source (FiberLite or Ocean Optics HL-2000) and a spectrometer (Ocean Optics USB2000 or Oriel MS127i, InstraSpec IV CCD). The intensity of the SS reflectance measurements are calibrated to the FD values of absorption and scattering to establish the absolute reflectance intensity. Absorption spectra were extracted from the absolute SS reflectance spectra by subtracting the scattering contribution across the spectral range of interest using a power-law fit of FD scattering coefficient measurements. Finally, the tissue concentrations of oxyhemoglobin ($HbO_2$), deoxyhemoglobin (Hb-R), MetHb, $H_2O$, and MB are calculated by a linear least squares fit of the wavelength-dependent extinction coefficient spectra of each chromophore. We used $HbO_2$, Hb-R, and MetHb extinction spectra reported by Zijlstra et al. (42) for the subsequent fitting and analysis.

*Animal model.* Pathogen-free New Zealand White rabbits (Myrtle Rabbitry, Thompson Station, TN), weighing ~3.5–4.1 kg, were used. Animals were housed in a pathogen-free animal facility and were given a commercial basal diet and water ad libitum. The study was approved by the Institutional Laboratory Animal Care and Use Committee, University of California, Irvine (ARC protocol no. 2000-2218).

*Measurement procedures.* The animals were initially sedated by an intramuscular injection of the mixture of ketamine HCl (100 mg/ml, Ketaject, Phoenix Pharmaceutical, St. Joseph, MI) and xylazine (20 mg/ml, Anased, Lloyd Laboratories, Shenandoah, IA) at a dose of 0.75 ml/kg. The animals' body weight and temperature were assessed after sedation. A 22-gauge catheter was then placed and secured into the animals' marginal ear veins for the subsequent intravenous anesthesia injection. The animals were then immediately intubated with a 3.0 cuffed endotracheal tube and placed on mechanical ventilation (dual-phase-control respirator, model 32A4BEPM-5R, Harvard Apparatus, Chicago, IL) with the following settings: tidal volume 50 ml, respiratory rate 25 breaths/min, and 100% oxygen fraction. Blunt dissection was performed to isolate the femoral artery on the left thigh slightly distal to the inguinal ligament, and a 20-gauge catheter was secured within the femoral artery for systemic blood pressure measurements and arterial sampling. Pressure measurements were obtained with a calibrated pressure transducer (TSD104A Transducer and MP100 WSW System, Biopac Systems, Santa Barbara, CA).

A plastic probe incorporating the source and detector fibers was placed on the medial surface of the right hind thigh for the broadband

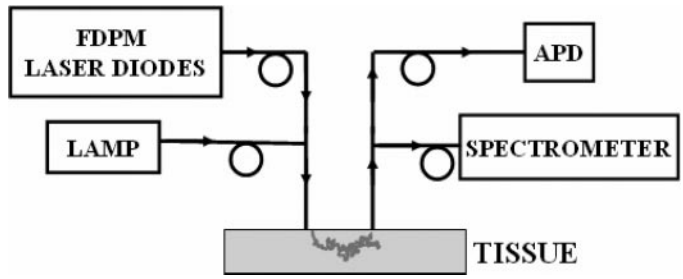


Fig. 2. Schematic diagram of broadband diffuse optical spectroscopy (DOS). FDPM, frequency domain photon migration; APD, avalanche photo diode.

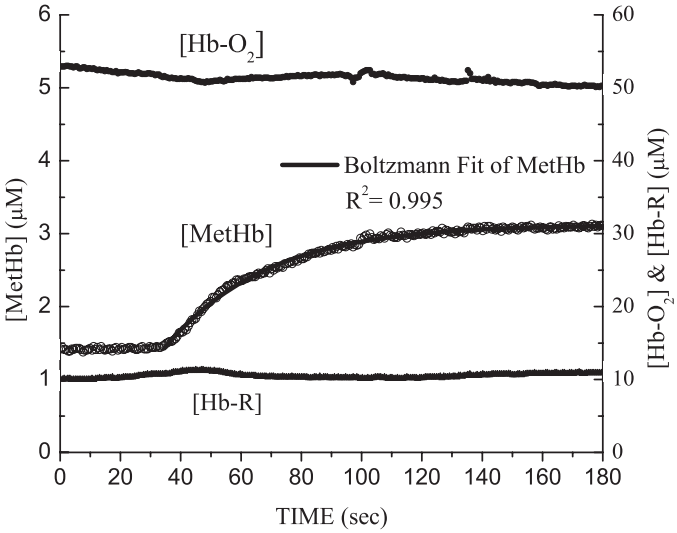


Fig. 3. Formation of MetHb with 0.1 ml amyl nitrite bolus into the right ear vein of the rabbit; the oxidation of $HbO_2$ to MetHb is apparent from the plot, whereas the concentration of Hb-R increased less than 1%. Brackets denote concentration.

DOS measurements. A source and detector separation of 10 mm was used for both FD and SS acquisitions. The reduced scattering coefficients were acquired from FD measurements at the discrete diode laser wavelengths and fit before $NaNO_2$ (or AN) bolus injection. To optimize the measurement speed, we first established that the changes in scattering coefficients at FD wavelengths and the scattering slopes were within 5% of the baseline values during the entire procedure. Therefore, we assumed that the long-term changes in tissue that could affect scattering were minimal compared with nitrite- and MB-induced variations in absorption spectra (which can be up to 60% changes from baseline). SS measurements were performed every 750 ms during the entire measurement sequence.

After various levels of $NaNO_2$ doses were tried, the optimal $NaNO_2$ (500 mg/60 ml normal saline) dosage was determined experimentally and administrated at a rate of 2.6 ml/min to allow for blood draws and titration of fluids and vasopressors for hemodynamic support. Arterial blood samples were obtained every 5–10 min until the blood obtained appeared visibly darker. At that point MB solution [15 mg/60 ml normal saline (NS)] were then infused five times over ~1.27 min each time, at a rate of 7.9 ml/min. After each 10-ml infusion, arterial blood sampling was collected and MB infusion resumed. Both MB and $NaNO_2$ were infused using an automated infuser. Norepinephrine (4 mg/500 ml NS) was titrated to maintain systolic blood pressure above 80 mmHg. Animals that developed distress or survived the induction and reversal of methemoglobinemia were euthanized by standard procedures at the end of studies (pentobarbital sodium, Eutha-6, intravenous injection).

Currently, cooximetry is considered the gold standard in monitoring methemoglobinemia. To validate the clinical use of broadband DOS, %MetHb results from broadband DOS need to be evaluated in the context of cooximetry. The on-site cooximetry measurements (AVOXimeter 4000, AVOX Systems, San Antonio, TX) were conducted on four rabbits during different stages of MetHb induction to avoid possible discrepancy due to continued blood oxidation. Because there is spectral overlap between MetHb and MB, these cooximetry measurements were done only during induction stages to ensure accuracy of cooximetry results.

*Drug kinetics.* Indirect oxidation of hemoglobin involves a process of cooxidation in which AN or sodium nitrite is cooxidized with heme

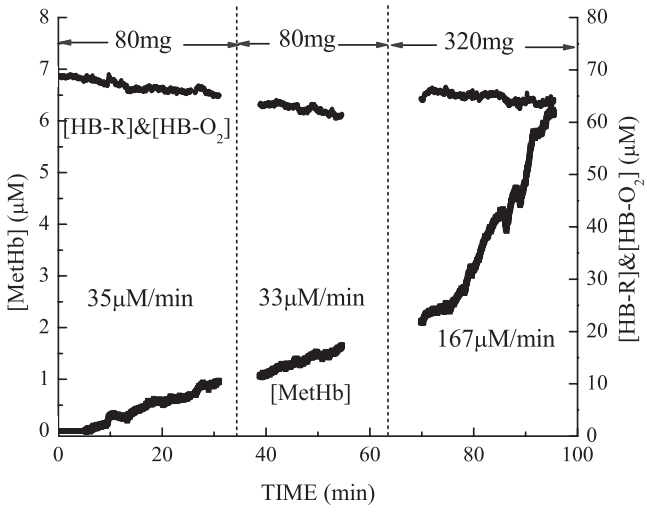


Fig. 4. Induction of MetHb with sodium nitrite. First two segments are with $NaNO_2$ concentration of 80 mg/60 ml each, and the last segment is with the concentration of 320 mg/60 ml.

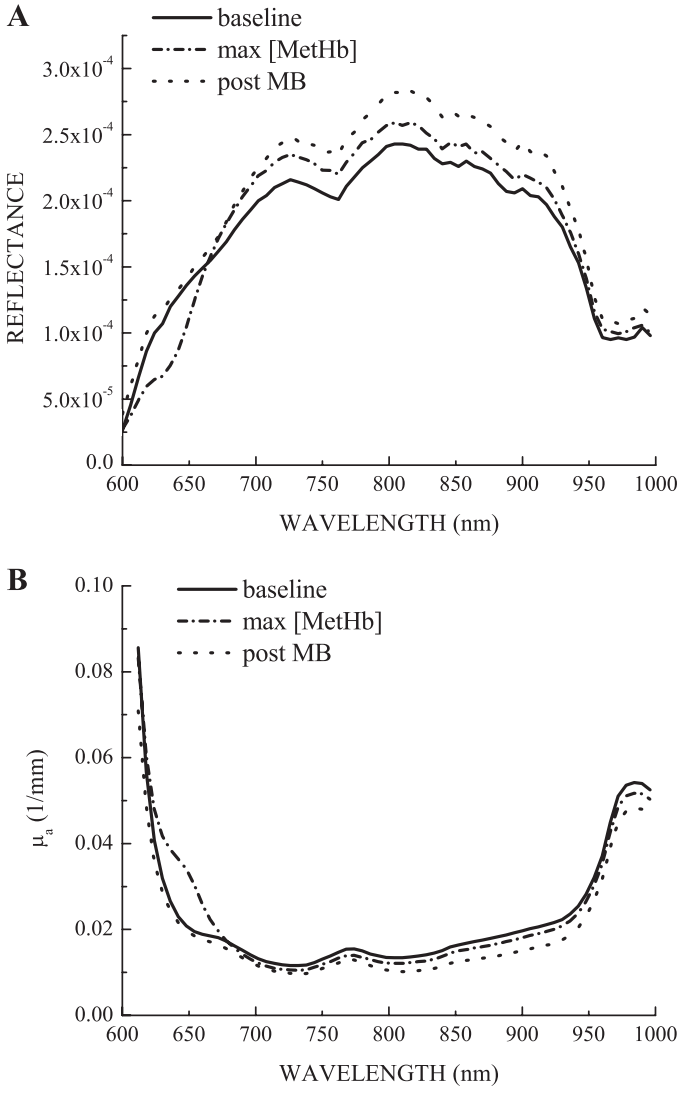


Fig. 5. Calibrated reflectance (*A*) and absorption spectra ($\mu_a$; *B*) of *rabbit 1*; straight line represents spectra at the baseline, dash dotted line at the maximum [MetHb], and dotted line at the end of MB treatment.

iron by $HbO_2$. The mechanism of nitrite-induced oxidation has been studied extensively, because nitrites are an important cause of toxic methemoglobinemia. The oxidation of hemoglobin is recognized as an autocatalytic process by nitrites. Because nitrite is a univalent reductant of $O_2$, the overall pathway generally involves the reduction of oxygen to superoxide ($O_2^-\cdot$) and hydrogen peroxide ($H_2O_2$).

For cases of methemoglobinemia resulting from drug exposure, MB is infused as the treatment, whose action depends on the availability of reduced nicotinamide adenine nucleotide phosphate (NADPH) within the red blood cell. NADPH reductase reduces MB to leukomethylene blue (LMB), which acts as an electron donor, and MetHb is reduced back to hemoglobin.

## RESULTS

MetHb was successfully induced with a 0.1 ml AN bolus. Figure 3 shows the concentration changes of $HbO_2$, Hb-R, and MetHb after AN injection. The mean [MetHb] before AN injection was 1.42 ± 0.02 μM, which represents the baseline endogenous [MetHb] (where brackets denote concentration). The maximum increase in [Hb-R] was less than 1%, whereas the [MetHb] increased from baseline to 3.17 μM. It represents 2.2 and 4.85% of the total hemoglobin concentration, respectively. There was a concurrent decrease in [$HbO_2$] (~1.75 μM) during the MetHb formation. The sensitivity of the measurement was established by fitting the [MetHb] vs. time plot in Fig. 3 with a Boltzmann function ($R^2 = 0.995$) and calculating the standard deviation of measurement data points from the fitting function (SD = 29.4 nM). As a result, it was determined that broadband DOS was able to detect as little as 30 nM [MetHb] changes in tissue.

Figure 4 illustrates the induction of MetHb utilizing two different concentrations of sodium nitrite ($NaNO_2$) solution. During the initial part of the study, 80 mg (in 60 ml, NS) was administrated twice intravenously over the same time duration. Broadband DOS detected ferric oxidation at a rate of 35 and 33 μM/min, respectively. Quadrupling the dose (320 mg/60 ml NS) while administering $NaNO_2$ over a similar time duration resulted in a corresponding formation rate increase at 167 μM/min. To maintain mean arterial blood pressure against the relaxation of small vessels by $NaNO_2$, Levophed (noreopinephrine bitartrate) had to be titrated between 4 and 16 μg/min to keep blood pressure above 80 mmHg.

After establishing a stable MetHb induction model using $NaNO_2$, we attempted the reduction of MetHb with 15 mg of MB (60 ml NS) after the intravenous administration of 500 mg $NaNO_2$ (60 ml NS) in three rabbits. Changes in the absolute reflectance and absorption coefficient, $\mu_a$, at the baseline (straight line), at the maximum MetHb concentration (dash-dotted line), and after MB treatment (dotted line) are shown in Fig. 5. Most significant spectral changes in both reflectance (Fig. 5*A*) and $\mu_a$ (Fig. 5*B*) occurred at the MetHb absorption

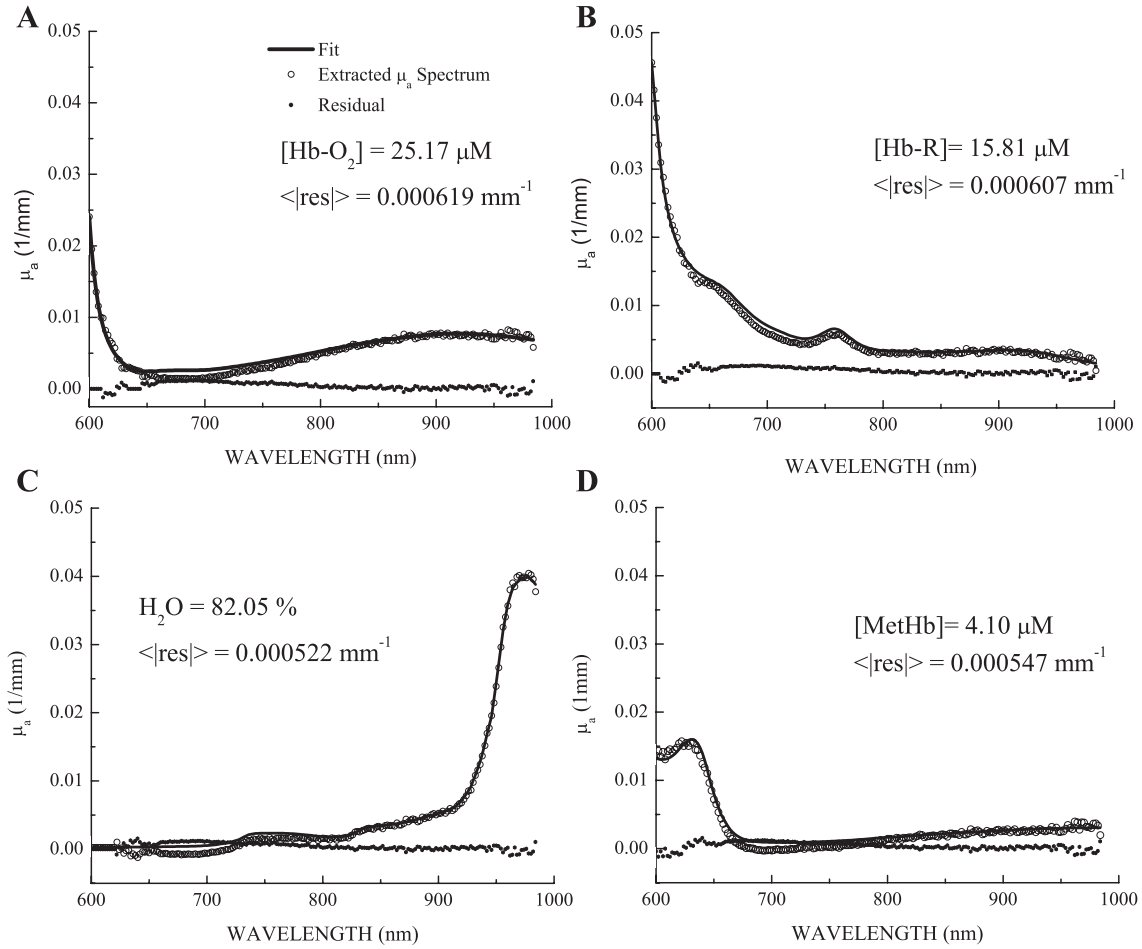


Fig. 6. Comparison between extracted $\mu_a$ spectrum and broadband DOS $\mu_a$ fit of individual chromophores at the maximum [MetHb] shown in Fig. 5. The average values of absolute residuals, <|res|>, are listed in each figure. *A*: $HbO_2$. *B*: Hb-R. *C*: water. *D*: MetHb.

peak of 630 nm. At the peak MetHb concentration, reflectance value at 630 nm decreased 37.3% from baseline value and returned within 10% of baseline after MB treatment. Likewise, the absorption coefficient increased 58.1% from baseline at the peak MetHb concentration, returning to within 7% of baseline post MB treatment at 630 nm. Figure 6 shows the extracted $\mu_a$ spectrum, broadband DOS $\mu_a$ fit, and fitting residual of individual chromophores at the maximum [MetHb]. The $\mu_a$ spectrum was extracted by subtracting absorption contributions of other chromophores from the measured absorption spectrum shown in Fig. 5*B*. The broadband DOS $\mu_a$ fit of each chromophore is the product of the extinction coefficient shown in Fig. 1 and the respective tissue concentrations. The average values of absolute residuals, $<|res|>$, were used to compare the quality of the $\mu_a$ fit. They are 0.000619, 0.000607, 0.000522, and 0.000547 $mm^{-1}$ for $HbO_2$, Hb-R, $H_2O$, and MetHb, respectively. Figure 7 shows the in vivo time course concentration changes in MetHb, Hb-R, and $HbO_2$ measured by broadband DOS. Figure 7*A* clearly shows the increase in MetHb concentration during $NaNO_2$ administration and the subsequent decrease during MB treatment. These changes are consistent with the changes in absolute reflectance and $\mu_a$ shown in Fig. 5. The total hemoglobin concentration (THC; sum of Hb-R, $HbO_2$, and MetHb) is also shown in Fig. 7*A*. In Fig. 7*B*, [$HbO_2$] decreased once the $NaNO_2$ injection started as the conversion from $HbO_2$ to MetHb took place.

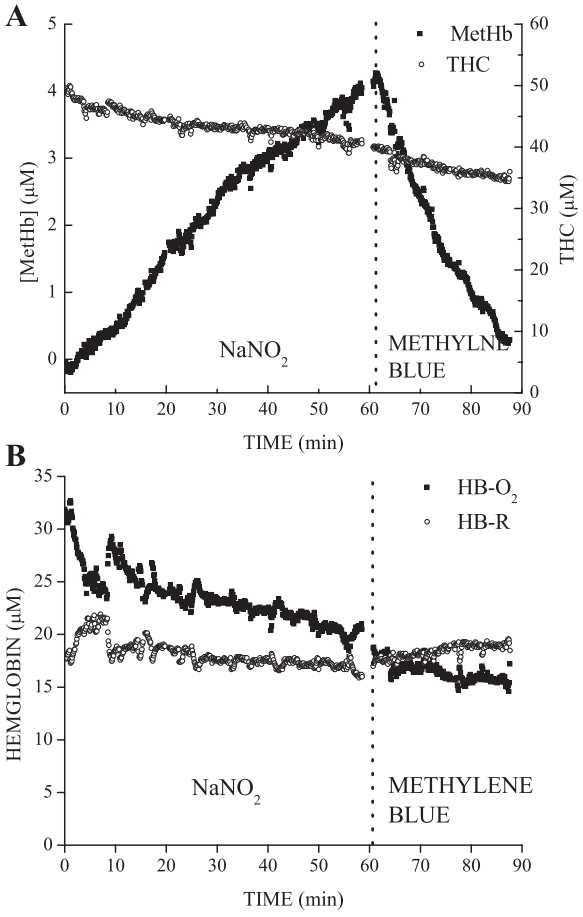


Fig. 7. In vivo time course concentration changes in total hemoglobin concentration (THC), MetHb (*A*), Hb-R, and $HbO_2$ (*B*) $NaNO_2$ and MB intervention in *rabbit 1*.

Table 1. *Concentrations of Hb-R, $HbO_2$, and MetHb measured by broadband DOS*

| | Weight, kg | $NaNO_2$, mg | MB, mg | | $HbO_2$, μM | Hb-R, μM | MetHb, μM |
|---|---|---|---|---|---|---|---|
| *Rabbit 1* | 4.1 | 300 | 15 | Base | 27.45 | 19.85 | 0.00* |
| | | | | Max | 18.04 | 17.65 | 4.22 |
| | | | | End | 15.60 | 19.06 | 0.30 |
| *Rabbit 2* | 3.5 | 150 | 12.5 | Base | 35.36 | 18.99 | 0.00* |
| | | | | Max | 26.40 | 17.67 | 4.03 |
| | | | | End | 17.88 | 19.88 | 0.00 |
| *Rabbit 3* | 4.2 | 250 | 15 | Base | 31.27 | 22.04 | 0.00* |
| | | | | Max | 26.22 | 18.09 | 4.38 |
| | | | | End | 18.96 | 22.00 | 0.00* |

Base, the baseline measurement prior to $N_aNO_2$ injection; Max, measurement point where methemoglobin concentration ([MetHb]) is the highest; End, after methylene blue (MB) treatment. Dosages of both $NaNO_2$ and MB noted here are the total amounts injected to the particular rabbits. Hb-R, deoxy hemoglobin; $HbO_2$, oxyhemoglobin; DOS, diffuse optical spectroscopy. Data were analyzed with the positive constraint on the chromophore concentrations.

Unlike the induction with AN in Fig. 3, the decreasing trend in the THC was much more noticeable with $NaNO_2$ injections. Hemodilution from fluid resuscitation and large $NaNO_2$ diluent volume is the most likely origin of this decrease in THC. Using the hemoglobin concentration data (g/dl) obtained from cooximetry, estimated initial blood volume (~50 ml/kg), and the amount of saline infused, it was estimated that THC would decrease approximately by 15.16, 9.33, and 12.50%, respectively for *rabbits 1*, *2*, and *3*. Table 1 summarizes the comparable decreases in THC (sum of Hb-R, $HbO_2$, and MetHb concentration) at 15.65, 11.49, and 8.68% from broadband DOS measurements, respectively.

Figure 8 shows the time-course change of MB concentration during the reduction of MetHb. The concentration plot clearly shows the five discrete injection points of MB and the extravasation. MB uptake and extravasation rates were extracted by linearly fitting each segment after MB bolus injections. Also, to estimate the utilization of each MB injection and kinetic rates of [MetHb] reduction, [MetHb] plots during five MB extravasation segments were fitted to a first-order exponential decay. Calculated decay constants, $\tau$ for MetHb decay and rates of MB uptake and extravasation are summarized in Table 2. Uptake rates of MB decreased from 210 to 64 nM/min after

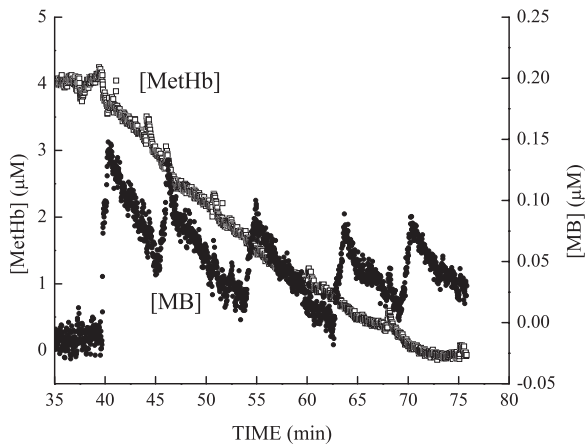


Fig. 8. Time-course concentration plots of MetHb and MB during reduction phase after MB bolus.

Table 2. *MB uptake and extravasation rates and MetHb decay rates during 5 MB injections*

| MB Injection | MB Uptake, nM/min | MB Extravasation, nM/min | MetHb Decay τ, min |
|---|---|---|---|
| *1* | 210 | −17 | 20.6 |
| *2* | 96 | −11 | 17.5 |
| *3* | 68 | −11 | 13.7 |
| *4* | 64 | −7 | 8.3 |
| *5* | 71 | −9 | 7.1 |

Uptake and extravasation rates of MB are calculated by linearly fitting MB concentration plots and decay time constants τ of MetHb were obtained with a single-exponential decay fitting.

each injection, and extravasation rates of MB also followed the same trend. [MetHb] decay constants of five segments also decreased from 20.6 min to 8.3 min, suggesting [MetHb] reduction rates are related to available [MetHb].

Overall MetHb decay kinetics of three rabbits were also calculated by fitting the broadband DOS decay plots in Fig. 9, employing a first-order exponential decay function {[chromophore] $\sim\exp(-t/\tau)$}. Respective decay constants, τ, and correlation coefficients, $r^2$, are noted in Fig. 10. The intrasubject variation in physiological response ranged from $\tau$ = 15.0 and 21.6 min (*rabbits 1* and *3*) to $\tau$ = 45.2 min in *rabbit 2*. These decay constants appeared to be related to MB dose and rabbit size.

In previous sections, we detailed the development of MetHb animal model and demonstrated that broadband DOS can monitor the oxidation of hemoglobin and the reduction of MetHb quantitatively. Figure 10 shows a very close correlation in all four rabbit measurements between broadband DOS and cooximetry values ($r^2$ = 0.902). Error bars on cooximetry results indicate the standard deviation of the repeated analysis of the same sample reported by the manufacturer (0.7%). Out of 21 measurement points, only three measurements resulted in the differences greater than 3% between broadband DOS and

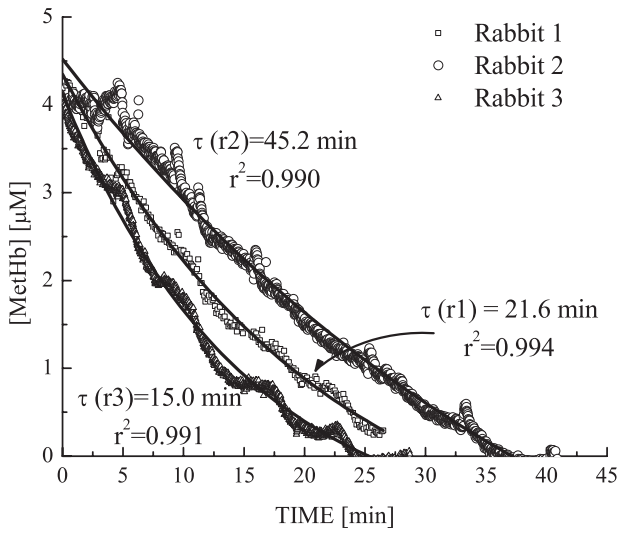


Fig. 9. Decay constant comparison of 3 rabbits when [MetHb] plots were fitted with single-exponential decay; *rabbits 1* and *3* were similar weight (4.1 and 4.2 kg) and given similar dosage of $NaNO_2$ and MB, whereas *rabbit 2* weighed less (3.5 kg) and was given lower dosage of $NaNO_2$ (150 mg) and MB (12.5 mg). τ, Decay constant.

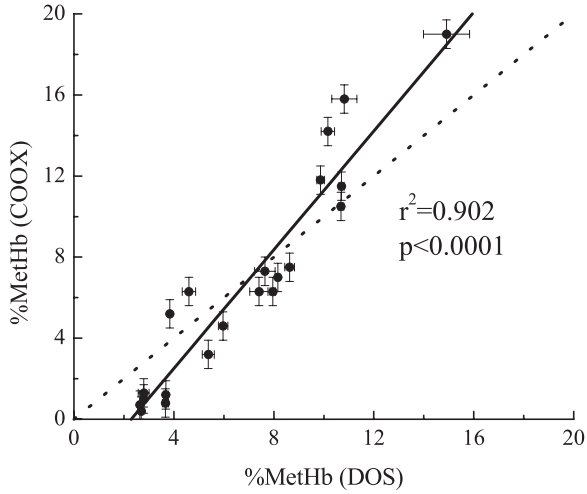


Fig. 10. Comparison of % MetHb between broadband DOS and on-site cooximetry (COOX) values in 4 rabbits. Because there is spectral overlap between MetHb and MB, these measurements were done only during induction stages to ensure accuracy of cooximetry results. A dotted line represents the line of identity. Error bars on cooximetry results indicate the standard deviation of the repeated analysis of the same sample reported by the manufacturer (0.7%).

cooximetry in %MetHb. In addition, using cooximetry as a reference measurement, further validation of broadband DOS measurements of MetHb was conducted to test the robustness of the fitting algorithm when other hemoglobin concentrations are changed. The validation experiment was carried out by modulating the fraction of inspired oxygen from 100 to 21% during different MetHb induction stages. The largest changes in arterial oxygen saturation, (from cooximetry), [Hb-R], and [$HbO_2$] were observed during the baseline measurements (18%, 4.1 μM, and 3.1 μM, respectively), whereas corresponding changes in [MetHb] and %MetHb were 0.06 μM and 0.1%, respectively. From this experiment, we conclude that changes in [Hb-R] and [$HbO_2$] do not induce artifacts in [MetHb].

## DISCUSSION

In vivo quantitative, noninvasive dynamic monitoring of biochemical processes is one of the most difficult and important challenges in medical diagnostics. Near-infrared spectroscopy (NIRS) has been widely employed for this purpose. However, conventional methods generally do not separate light absorption from scattering and, as a result, do not accurately report absolute biochemical concentrations in tissue. However, advances in light transport modeling and technology have allowed the separation of light scattering and absorption in tissue and have enabled quantitative approaches (3, 7, 12–15, 22, 23, 29, 31). In this study, we employ a quantitative method based on broadband DOS that combines multifrequency FDPM methods with NIRS. We demonstrate that broadband DOS can be used to dynamically monitor in vivo concentrations of multiple chromophores in tissue noninvasively. Particular emphasis is placed on DOS sensitivity to dynamic changes in chromophore concentrations and physiological information that can be used to assess the success of therapeutic interventions.

Broadband DOS is able to detect submicromolar changes in an exogenous therapeutic agent, MB, as well as $HbO_2$, Hb-R,

and MetHb dynamics. For example, during AN injection (Fig. 3), we observed rapid changes in hemoglobin states even at low concentration (~2.2% MetHb) and the conservation of THC during the autocatalytic oxidation process from $HbO_2$ to MetHb by nitrites. Percent MetHb (2.2%) detected by broadband DOS before AN injection is similar to the normal MetHb level (19). Unfortunately, AN caused fatal cardiovascular collapse on multiple occasions, despite yielding significant amounts of MetHb. Klimmek et al. (25) noted similar findings, reporting that half-maximum MetHb concentration occurred in less than 1 min and the natural reduction process started less than 5 min after the injection. AN with its inherent ability to rapidly oxidize hemoglobin and cause fatal hemodynamic shock leads us to the use of sodium nitrite in subsequent experiments. Nonetheless, with AN injection model, we obtained the maximum sensitivity range of broadband DOS measurements, owing to its fast reaction rate and the lack of physiological response by the animal.

Ccompared with the AN injection model, we were able to establish a stable animal model with $NaNO_2$ injection for the formation and reduction of MetHb. It should be noted that this $NaNO_2$ injection model is an "open" system involving multiple blood samplings, anesthesia injections, and fluid infusions to sustain animals for the longer time scale measurements. Figure 4 shows that broadband DOS tracks [MetHb] induced by different doses of $NaNO_2$. We were able to quantify the dose response of broadband DOS measurements by calculating in vivo formation rates of MetHb. This kind of in vivo rate kinetics is not available elsewhere, and it can be useful in the methemoglobinemia management, especially in assessing therapeutic drug delivery.

The sensitivity of DOS to MetHb formation and reversal using $NaNO_2$/MB was observed in a series of studies performed in three subjects. In contrast to AN administration (Fig. 3), the $NaNO_2$ injection model is an open system, and THC, [$HbO_2$], and [Hb-R] were not conserved. This is illustrated by the gradual decline in THC that is coincident with MetHb formation (Fig. 7*A*). In Fig. 7*B*, an increase in [Hb-R] is noted after MB treatment. The increase in [Hb-R] is believed to be mainly due to the reduction of MetHb to Hb-R via an enzymatic pathway involving NADPH and LMB. It is possible that [$HbO_2$] did not rebound after MB treatment because of the hemodilution effect from further saline infusion associated with MB injection (60 ml). However, physiological compensatory mechanisms could have been compromised severely owing to various external interventions, including $NaNO_2$, MB, and norepinephrine infusions. The fact that DOS provides additional physiological information such as an oxygen-carrying capacity besides quantitative monitoring of [MetHb] demonstrates the benefit of DOS in methemoglobinemia management.

The uptake and extravasation rates of MB were determined from Fig. 8 results by use of a simple linear fitting of concentration plots. A single exponential decay model was used for [MetHb] reversal in Figs. 8 and 9. These models provide a simple quantitative framework for comparing time-dependent changes in MetHb formation and reversal kinetics (Table 2). Variations in in vivo kinetics appear to be strongly associated with [MetHb] and its reversal by MB. For example, at the highest [MetHb], both uptake and extravasation rates of MB and decay constant, $\tau$, for MetHb decay are the highest, and they gradually decrease as [MetHb] declines.

Regardless of the precise kinetic model, these findings underscore the importance of broadband DOS as a potential platform for investigating in vivo drug utilization kinetics. As shown in Fig. 10, we have demonstrated the clinical feasiblity of broadband DOS in methemoglobinemia monitoring and diagnosis. As broadband DOS technology matures with further refinements, we expect that ultimately this approach could be used in a clinical setting to gain insight on therapeutic efficacy, particularly in the cases of cyanide toxicity treatment with therapeutically induced MetHb and in neonatal methemoglobinema management during inhaled nitric oxide treatment for hypoxemic respiratory failure.

The current limitation of broadband DOS and NIRS in general is the inability to distinguish between hemoglobin and myoglobin contributions. In fact, what is being measured is the combined concentration of hemoglobin and myoglobin species. However, the inability to separate myoglobin from hemoglobin will affect the absolute values measured, not the relative ones. The concentration of oxy- and deoxymyoglobin is not variable in the clinically relevant ranges of tissue $P_{O_2}$; hence the absorbance due to this chromophore is essentially constant (33).

## ACKNOWLEDGMENTS

We thank Terry Waite-Kennedy, Tanya Burney, and David Mukai for assistance with experiments.

## GRANTS

This work is based on research sponsored by the Air Force Research Laboratory, under agreement number FA9550-04-1-0101. The U.S. Government is authorized to reproduce and distribute reprints for Governmental purposes notwithstanding any copyright notation thereon. This work is also supported by Laser Microbeam and Medical Program, Beckman Laser Institute, University of California, Irvine (Grant no. 445574-30133).

## REFERENCES

1. **Alexander CM, Teller LE, and Gross JB.** Principles of pulse oximetry: theoretical and practical considerations. *Anesth Analg* 68: 368–376, 1989.
2. **Barker SJ, Tremper KK, and Hyatt J.** Effects of methemoglobinemia on pulse oximetry and mixed venous oximetry. *Anesthesiology* 70: 112–117, 1989.
3. **Bays R, Wagnieres G, Robert D, Braichotte D, Savary JF, Monnier P, and van den Bergh H.** Clinical determination of tissue optical properties by endoscopic spatially resolved reflectometry. *Appl Opt* 35: 1756–1766, 1996.
4. **Bevilacqua F, Berger AJ, Cerussi AE, Jakubowski D, and Tromberg BJ.** Broadband absorption spectroscopy in turbid media by combined frequency-domain and steady-state methods. *Appl Opt* 39: 6498–6507, 2000.
5. **Bucklin R and Myint MK.** Fatal methemoglobinemia due to well water nitrates. *Ann Intern Med* 52: 703–705, 1960.
6. **Craun GF, Greathouse DG, and Gunderson DH.** Methaemoglobin levels in young children consuming high nitrate well water in the United States. *Int J Epidem* 10: 309–317, 1981.
7. **Cubeddu R, Pifferi A, Taroni P, Torricelli A, and Valentini G.** Noninvasive absorption and scattering spectroscopy of bulk diffusive media: an application to the optical characterization of human breast. *Appl Phys Lett* 74: 874–876, 1999.
8. **Cuccia DJ, Bevilacqua F, Durkin AJ, Merritt S, Tromberg BJ, Gulsen G, Yu H, Wang J, and Nalcioglu O.** In vivo quantification of optical contrast agent dynamics in rat tumors by use of diffuse optical spectroscopy with magnetic resonance imaging coregistration. *Appl Opt* 42: 2940–2950, 2003.
9. **Da-Silva SS, Sajan IS, and Underwood JP 3rd.** Congenital methemoglobinemia: a rare cause of cyanosis in the newborn—a case report. *Pediatrics* 112: e158–e161, 2003.

10. **Delwood L, O'Flaherty D, Prejean EJ 3rd, and Giesecke AH.** Methemoglobinemia and its effect on pulse oximetry. *Crit Care Med* 19: 988, 1991.
11. **Evelyn K and Malloy H.** Microdetermination of oxyhemoglobin, methemoglobin, and sulfhemoglobin in a single sample of blood. *J Biol Chem* 126: 655–662, 1938.
12. **Fantini S, Franceschini MA, Maier JS, Walker SA, Barbieri B, and Gratton E.** Frequency-domain multichannel optical-detector for noninvasive tissue spectroscopy and oximetry. *Opt Eng* 34: 32–42, 1995.
13. **Farrell TJ, Patterson MS, and Wilson B.** A diffusion-theory model of spatially resolved, steady-state diffuse reflectance for the noninvasive determination of tissue optical-properties invivo. *Med Phys* 19: 879–888, 1992.
14. **Finlay JC and Foster TH.** Hemoglobin oxygen saturations in phantoms and in vivo from measurements of steady-state diffuse reflectance at a single, short source-detector separation. *Med Phys* 31: 1949–1959, 2004.
15. **Fishkin J, Coquoz O, Anderson E, Brenner M, and Tromberg B.** Frequency-domain photon migration measurements of normal and malignant tissue optical properties in a human subject. *Appl Opt* 36: 10–20, 1997.
16. **Fishkin JB, So PTC, Cerussi AE, Fantini S, Franceschini MA, and Gratton E.** Frequency-domain method for measuring spectral properties in multiple-scattering media - methemoglobin absorption-spectrum in a tissuelike phantom. *Appl Opt* 34: 1143–1155, 1995.
17. **Goldstein BD.** Exacerbation of dapsone-induced Heinz body hemolytic anemia following treatment with methylene blue. *Am J Med Sci* 267: 291–297, 1974.
18. **Graaff R, Aarnoudse JG, Zijp JR, Sloot PMA, Demul FFM, Greve J, and Koelink MH.** Reduced light-scattering properties for mixtures of spherical-particles - a simple approximation derived from Mie calculations. *Appl Opt* 31: 1370–1376, 1992.
19. **Hardy HL, and Boylen J GW.** Cyanogen, hydrocyanic acid and cyanides. In: *Encyclopaedia of Occupational Health and Safety* (3rd ed.), edited by Parmeggiani L. Geneva: International Labour Office, 1983, p. 574–577.
20. **Jakubowski DJ.** *Development of Broadband Quantitative Tissue Optical Spectroscopy for the Non-Invasive Characterization of Breast Disease* (PhD Thesis). Irvine: University of California, Irvine, 2002.
21. **Kern K, Langevin PB, and Dunn BM.** Methemoglobinemia after topical anesthesia with lidocaine and benzocaine for a difficult intubation. *J Clin Anesth* 12: 167–172, 2000.
22. **Kienle A, Lilge L, Patterson MS, Hibst R, Steiner R, and Wilson BC.** Spatially resolved absolute diffuse reflectance measurements for noninvasive determination of the optical scattering and absorption coefficients of biological tissue. *Appl Opt* 35: 2304–2314, 1996.
23. **Kienle A and Patterson MS.** Improved solutions of the steady-state and the time-resolved diffusion equations for reflectance from a semi-infinite turbid medium. *J Opt Soc Am A* 14: 246–254, 1997.
24. **Kirlangitis JJ, Middaugh RE, Zablocki A, and Rodriquez F.** False indication of arterial oxygen desaturation and methemoglobinemia following injection of methylene blue in urological surgery. *Mil Med* 155: 260–262, 1990.
25. **Klimmek R, Krettek C, and Werner HW.** Ferrihaemoglobin formation by amyl nitrite and sodium nitrite in different species in vivo and in vitro. *Arch Toxicol* 62: 152–160, 1988.
26. **May RB.** An infant with sepsis and methemoglobinemia. *J Emerg Med* 3: 261–264, 1985.
27. **Mourant JR, Fuselier T, Boyer J, Johnson TM, and Bigio IJ.** Predictions and measurements of scattering and absorption over broad wavelength ranges in tissue phantoms. *Appl Opt* 36: 949–957, 1997.
28. **Ohashi K, Yukioka H, Hayashi M, and Asada A.** Elevated methemoglobin in patients with sepsis. *Acta Anaesthesiol Scand* 42: 713–716, 1998.
29. **Patterson MS, Chance B, and Wilson BC.** Time resolved reflectance and transmittance for the noninvasive measurement of tissue optical-properties. *Appl Opt* 28: 2331–2336, 1989.
30. **Pham TH, Coquoz O, Fishkin JB, Anderson E, and Tromberg BJ.** Broad bandwidth frequency domain instrument for quantitative tissue optical spectroscopy. *Rev Sci Instrum* 71: 2500–2513, 2000.
31. **Pogue BW and Patterson MS.** Frequency-domain optical absorption spectroscopy of finite tissue volumes using diffusion theory. *Phys Med Biol* 39: 1157–1180, 1994.
32. **Rausch-Madison S and Mohsenifar Z.** Methodologic problems encountered with cooximetry in methemoglobinemia. *Am J Med Sci* 314: 203–206, 1997.
33. **Richards-Kortum R and Sevick-Muraca E.** Quantitative optical spectroscopy for tissue diagnosis. *Annu Rev Phys Chem* 47: 555–606, 1996.
34. **Rosen PJ, Johnson C, McGehee WG, and Beutler E.** Failure of methylene blue treatment in toxic methemoglobinemia. Association with glucose-6-phosphate dehydrogenase deficiency. *Ann Intern Med* 75: 83–86, 1971.
35. **Schmitt JM and Kumar G.** Optical scattering properties of soft tissue: a discrete particle model. *Appl Opt* 37: 2788–2797, 1998.
36. **Shauvall HI and Gruener N.** Health effects of nitrates in water. Washington, DC: EPA, 1977, p. 600.
37. **Sigell LT, Kapp FT, Fusaro GA, Nelson ED, and Falck RS.** Popping and snorting volatile nitrites: a current fad for getting high. *Am J Psychiatry* 135: 1216–1218, 1978.
38. **Singh RK, Kambe JC, Andrews LK, and Russell JC.** Benzocaine-induced methemoglobinemia accompanying adult respiratory distress syndrome and sepsis syndrome: case report. *J Trauma* 50: 1153–1157, 2001.
39. **Tromberg BJ, Shah N, Lanning R, Cerussi A, Espinoza J, Pham T, Svaasand L, and Butler J.** Non-invasive in vivo characterization of breast tumors using photon migration spectroscopy. *Neoplasia* 2: 26–40, 2000.
40. **Udeh C, Bittikofer J, and Sum-Ping ST.** Severe methemoglobinemia on reexposure to benzocaine. *J Clin Anesth* 13: 128–130, 2001.
41. **Wright RO, Lewander WJ, and Woolf AD.** Methemoglobinemia: etiology, pharmacology, and clinical management. *Ann Emerg Med* 34: 646–656, 1999.
42. **Zijlstra WG, Buursma A, and Assendelft OW.** *Visible and Near-infrared Absorption Spectra of Human and Animal Hemoglobin: Determination and Application*. Zeist, Netherlands: VSP, 2000.